Performance improvement of solar still by using hybrid nanofluids

Hossain Md. Fazle Rabbi[1] · Ahmet Z. Sahin[1]

Abstract

The biggest shortcoming of conventional solar still is its limited productivity. In this work, improvement of solar still performance using two hybrid nanofluids is examined. Use of hot water and two conventional nanofluids were also utilized to study the improvement of the performance of solar still. Hybrid nanofluids, hot water or conventional nanofluids were linked to the solar system with heat exchanger placed at the bottom of the basin of the solar still. Pure desalinated water yield, the first and the second law efficiencies of the solar still with hybrid nanofluid were observed through modeling. Utilization of heat exchanger with hot water improved the solar still performance. Conventional nanofluids showed better performance than hot water. The best performance is obtained with the use of hybrid nanofluids. The yield, thermal efficiency and exergy efficiency with water–Al_2O_3–SiO_2 hybrid nanofluid resulted in 4.99 kg m^{-2} day^{-1}, 37.76% and 0.82%, respectively. The basin water depth, nanofluid flow rate, inlet heat exchanger temperature of the nanofluid and nanoparticle concentration played vital role together with solar radiation and ambient temperature to improve the performance.

Keywords Solar still · Nanofluid · Hybrid nanofluid · Performance · Efficiency

Introduction

The conquest of finding safe drinking water has been going on since old times. One of the simplest techniques of producing freshwater is solar desalination in solar still. The technological simplicity, use of abundantly available solar energy and low cost make it a popular choice for the people of remote locations specially in less developed countries [1]. Conventional solar still has very low productivity and very poor thermal performance due to convective and radiative heat losses. Use of nanofluid is one of the most notable ways of overcoming these shortcomings. Usage of nanofluid is found in numerous cases in the literature for analyzing free or natural convection, energy and exergy of different systems and different solar energy applications, etc. [2–6]. Nanofluids, prepared by adding nanometer-sized additives in base fluid, possess better thermophysical and optical properties to make better heat transfer and reduced heat loss to produce more fresh water. Heat transfer coefficients are increased by using nanofluids which in turn increases

the production of solar still. That is why nanofluids are being used in solar still nowadays to improve the production rate and the thermal performance together with some other modifications like adding condenser, heat exchanger, wicks, vacuum system, evacuated tube, etc. [7–9]. Use of Nanofluid in producing fresh water from the salty sea water is very beneficial for the environment too. It was found out that the use of copper oxide–water nanofluid reduces significant amount of carbon dioxide [10]. These are the reasons of using nanofluids extensively in various energy related fields such as domestic refrigeration, absorption system, thermal management of different electronic equipment, medicine, building heating and cooling, etc. although the preparation cost of nanofluids is quite high [11, 12]. It was experimentally found that the use of copper oxide (Cu_2O) nanofluid with external Thermoelectric glass cover cooling channel enhances the performance of solar still significantly. With this modification, varying the volumetric amount of nanofluid results in higher amount of pure water from brackish water, better energy efficiency and better exergy efficiency compared to conventional solar stills. The performance with the improved solar still shows that the production of water, energy efficiency and the second law efficiency increases by 81%, 80.6% and 112.5%, respectively [13]. In another study with Cu_2O nanofluid with an external thermoelectric

✉ Ahmet Z. Sahin
azsahin@kfupm.edu.sa

1 Mechanical Engineering Department, King Fahd University of Petroleum and Minerals, Dhahran, Saudi Arabia

condensing channel also resulted in very high efficiency of the solar still. Addition of 0.08% volume fraction of this nanoparticle, the yield of pure water, first law and second law efficiencies were enhanced by about 82.4%, 81.5% and 92.5%, respectively [14]. In another study of solar still with external condenser with mass concentration of 0.02–0.03% Cu_2O and Al_2O_3 nanoparticles resulted in daily efficiency of 84.16% and 73.85%, respectively. The daily efficiency of conventional still was only 34% [15]. Fresh water production increases by 116% using Aluminum oxide–water nanofluid with external condenser [16]. A VOF (volume of Fluid) model was utilized to study the heat transfer phenomenon and the performance of a solar still using Al_2O_3–water nanofluid. The findings showed that the productivity increases about 25%, Nusselt number increases about 18% when the solid volume fraction of the nanoparticles increased from 0 to 5% [17].

Arrangement of vacuum creation together with nanofluids also increases the solar still performance significantly. Cuprous oxide nanoparticles (concentration of 0.2%) with vacuum and without vacuum increased freshwater production by 133.64% and 93.87%, respectively. 125% and 88.97% increase of distillate production recorded for the case of Al_2O_3 nanofluid [18]. Using Al_2O_3–Therminol 55 (nHTF), nanofluid with a modified solar still with a Fresnel lens concentrator with evacuated tube receiver demonstrates remarkable improvement. It was experimentally found out that hourly production of fresh water to be 45–250.27% more than the conventional solar still using 0.1% nHTF nanofluid. Total yield was found 12.19 L m^{-2} day^{-1} which is much higher than conventional solar still producing only 3.48 L m^{-2} day^{-1}. The maximum efficiency found was 53.55% with this nanofluid [19]. Hybrid solar still with bottom basin single sloped and upper basin double sloped with $MgCl_2$ as regenerator and ZnO nanoparticles was constructed and the performance showed pure water yield of 623.33 mL m^{-2} and overall thermal efficiency of 19.20% [20]. Graphite and Copper oxide micro-flakes were utilized in varying concentrations as nanoparticles in water. The productivity with these nanofluids showed 53.95% and 44.91% more than the conventional simple solar still, respectively. With the use of glass film cooling by water together with these nanofluids improved productivity by 57.60% and 47.80%, respectively. The conventional solar still showed only 30% of productivity [21]. The performance of different nanofluids was also investigated in the case of pure water production from a solar still. The solar still with different nanofluids is compared to a conventional water solar still. The result shows that the still with Al_2O_3 nanofluid has 29.95%, with ZnO has 12.67% and with SnO_2 has 18.63% higher production than conventional solar still [22].

In another analytical study (modeling) of solar still with heat exchanger together with SiO_2–water and Cu–water nanofluids, freshwater yield, first law and second law efficiencies improved when inlet heat exchanger temperature of nanofluid was more than 60 °C. At lower temperature, solar still with Cu–water nanofluid showed better result than SiO_2–water nanofluid. But, with the inlet heat exchanger temperature more than 60 °C, SiO_2–water nanofluid showed higher yield, higher thermal and exergy efficiency than the Cu–water nanofluid. However, both the nanofluids performed much better than convention solar still at higher temperature. The mass flow rate and concentration of the nanoparticles also have noticeable impact on the performance of the solar still [23].

Traditional Pyramid Distiller (TPD) is a solar still in the shape of a pyramid. The performance of TPD increases with the addition of V corrugated absorbers and with the combination of both V corrugated materials and wick materials. The performance of TPD is even further increased with the addition of CuO nanoparticles with the wick materials. This addition of CuO nanoparticles together with the wick materials increased the productivity of fresh water, thermal efficiency and exergy efficiency by 72.95%, 77.9% and 93%, respectively, compared to TPD [24]. Thermoelectric heating (TEH) in the basin, TEH together with Silver nanofluid and combination of TEH, Silver nanofluid and external condenser were used separately to check the performance of solar still. The yield of pure water and thermal efficiency of solar still with nanofluid together with condenser showed 100.5% and 26.7% improvement than the solar still without both nanofluid and condenser. Even, the solar still with nanofluid without condenser also showed 50.8% and 30.6% improvement for yield and thermal efficiency, respectively, in comparison with traditional solar still [25]. Environment friendly coffee-based colloid was also used as nanofluid to boost the production of pure desalinated water. The experimental results showed the increase of yield of fresh water, thermal efficiency and exergy efficiency by 35.14%, 35.34% and 46.44%, respectively, compared to traditional solar still [26]. Evacuated tubes together with CuO and Carbon black (CB) nanoparticles are integrated with Conventional Pyramid Solar Still (CPSS) to make the Modified Pyramid Solar Still (MPSS). Fresh water yield of MPSS with CuO resulted in 54.48% and 27.85% higher production than Conventional Solar Still (CSS) and CPSS, respectively. Again, the production of yield of MPSS with CB was 57.098% and 33.59% higher than the CSS and CPSS, respectively. The efficiency of MPSS reached to 61% and 64% with CuO and CB, respectively [27].

Thus, it can be said that the performance improvement of the solar still using nanofluid is obvious. However, the selection of the appropriate nanofluid for the highest production and efficiency is not yet decided. The research is being carried out to find out the maximum possible efficiency of the solar still desalination system. One of the areas of study

to maximize efficiency of solar still is the utilization of various nanofluids.

In this paper, we aim at finding out the pure water yield and efficiency of a modified solar still using hybrid nanofluids. Because of possessing better properties than the conventional nanofluids, much better performance is expected from the solar still with hybrid nanofluids.

Mathematical modeling

Schematic representation of the solar still

The solar still considered in this work is equipped with a heat exchanger underneath the feed water (saline or impure water) as shown in Fig. 1. Hot water, conventional nanofluid or hybrid nanofluid flows through the heat exchanger to exchange heat with the feed water. However, the nanofluid does not mix with the water as the nanofluid flows through the tubes of the heat exchanger. A heater is used to heat the nanofluid before entering the heat exchanger. The schematic view of the heat exchanger inside the solar still is shown schematically in Fig. 2. We considered length of solar still, $L_{ss} = 1$ m and width of solar still, $W_{ss} = 0.85$ m for our study. Depth of water (d_w) of the solar still is varied to observe the change of performance. The input parameters used in the present analysis are the hourly solar radiation intensity, temperature of surrounding atmosphere, speed of wind at

the location and nanofluid temperature at the inlet of heat exchanger (T_{iHE}). On the other hand, the depth of water (d_w), nanofluid flow rate (m) and concentration of nanofluid are also some key parameters playing vital role to produce fresh condensed water in the analysis.

Following assumptions are considered while analyzing the current solar still system [8].

- There is no vapor or water leakage from the system
- The temperature of all the layers of basin water is considered same for any fixed period of time
- There is no heat absorption on the outer surface of the glass cover
- The processes in this system are considered to be quasi steady state
- The nanofluid is stable with well dispersed nanoparticles without any sedimentation

Thermodynamic analysis

The present model of the modified solar still consists of first law and second law analysis. Here, various mathematical equations are presented for energy balance at different parts of the system. The main parts of the system are the sloped glass, basin water, heat exchanger and basin liner. Although the evaporation heat transfer coefficient is the dominant factor to produce distilled water; conduction, convection and radiation heat transfer coefficients also play important role.

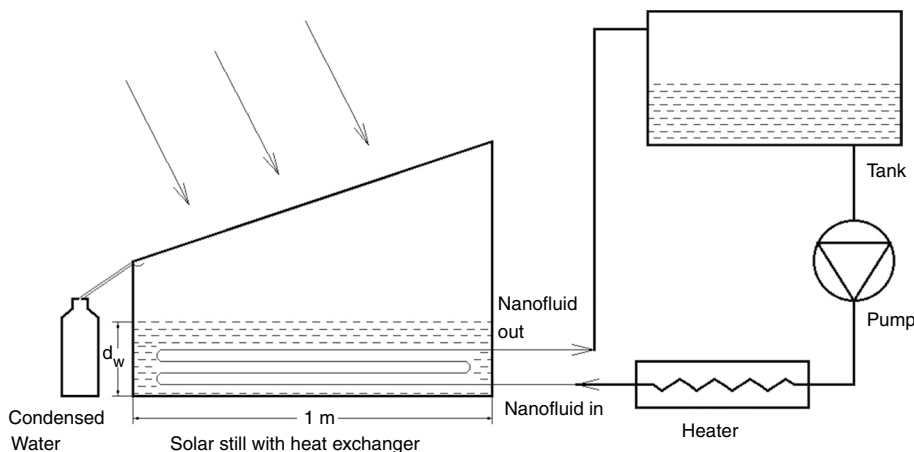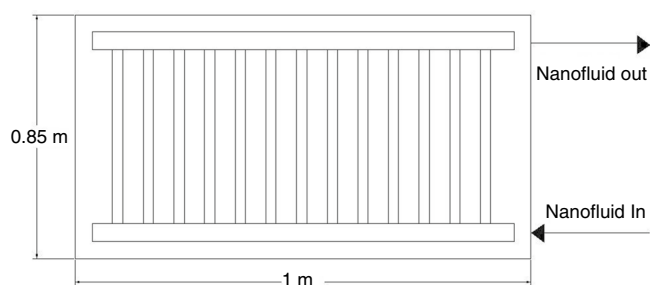**Fig. 1** Schematic diagram of solar still system

Fig. 2 Solar still with heat exchanger (top view)

Schematic diagram of the electrical analogy for the heat transfer in and out of the Solar Still is visualized in Fig. 3.

First law of thermodynamics analysis

First law of thermodynamics includes equations of energy balance for specific components of the solar still system. The equations of energy balance for various components of the system are described in the following paragraphs.

Glass cover outer surface The heat reaching the outer surface of the glass cover from the inner surface equals to the amount of heat going from the outer surface to the environment. It is considered that heat is not stored at the outer face of the glass cover

$$q_1 = q_2 \tag{1}$$

where

$$q_1 = h_{t,g,o-a}\left(T_{g,o} - T_a\right) \tag{2}$$

$$q_2 = \frac{k_g}{L_g}\left(T_{g,i} - T_{g,o}\right) \tag{3}$$

$$h_{t,g,o-a} = 5.7 + 3.8 V_w \tag{4}$$

q_1 reflects heat transfer from the external surface of glass cover to the atmosphere and q_2 denotes heat transfer from inside surface to the outer surface of the glass cover. k_g is thermal conductivity of glass, L_g is the thickness of the glass, T is temperature. $h_{t,g,o-a}$ is the total heat transfer coefficient from outer surface of glass to ambient. Subscript i, o, a, t, g

Fig. 3 Schematic view of the electrical analogy for the heat transfer in and out of the solar still

means inner, outer, ambient, total, and glass, respectively. V_w means wind velocity.

Inner surface of glass cover Solar radiation reaches the face of the glass, and some of the incident energy is absorbed in the inner surface. Some heat comes to the interior face of the glass cover from basin water. This phenomenon can be expressed as Eqs. (5–7) [28]

$$q_2 = q_3 + q_{abs,2} \tag{5}$$

here,

$$q_{abs,2} = \left(1 - R_g\right)\alpha_g I_s(t); \tag{6}$$

$$q_3 = \left(h_{r,wgi} + h_{ev,wgi} + h_{c,wgi}\right)\left(T_w - T_{g,i}\right); \tag{7}$$

The heat absorbed in the inside surface of glass from hourly solar radiation is $q_{abs,2}$. The heat reaching the glass inner surface from the water is q_3. All temperatures here are in kelvin unit. Heat transfer coefficient is denoted by h. Subscripts r, ev, c, wgi means radiation, evaporation, conduction and water to inner glass surface, respectively. R, α, I_s and P stands for reflectivity, absorptivity, hourly solar radiation intensity and pressure, respectively. Stefan Boltzmann constant and emissivity are marked with σ and ε, respectively. The evaporation heat transfer coefficient is estimated using the Dunkle relation stated in Eq. (8). Radiation and conduction heat transfer coefficients can be found from Eqs. (9) and (10) below [23]

$$h_{ev,wgi} = 0.016273 * h_{c,w-g,i}\left(\frac{P_w - P_{g,i}}{T_w - T_{g,i}}\right) \tag{8}$$

$$h_{r,wgi} = \sigma\left(T_w^2 + T_{g,i}^2\right)\left(T_w - T_{g,i}\right)\left[\frac{1}{\varepsilon_w} + \frac{1}{\varepsilon_g} - 1\right]^{-1} \tag{9}$$

$$h_{c,wgi} = 0.884\left[\left(T_w - T_{g,i}\right) + \frac{(P_w - P_{g,i})T_w}{268,900 - P_w}\right]^{1/3} \tag{10}$$

Here, P_w and P_{gi} are the saturated vapor pressure of water at temperature of water and inner surface of glass, respectively, which can be found out using Eqs. (11) and (12)

$$P_w = \exp\left(25.317 - \frac{5144}{T_w}\right) \tag{11}$$

$$P_{g,i} = \exp\left(25.317 - \frac{5144}{T_{g,i}}\right). \tag{12}$$

Water of the basin The water of the solar still absorbs the incident solar radiation, the useful heat gain from the heated
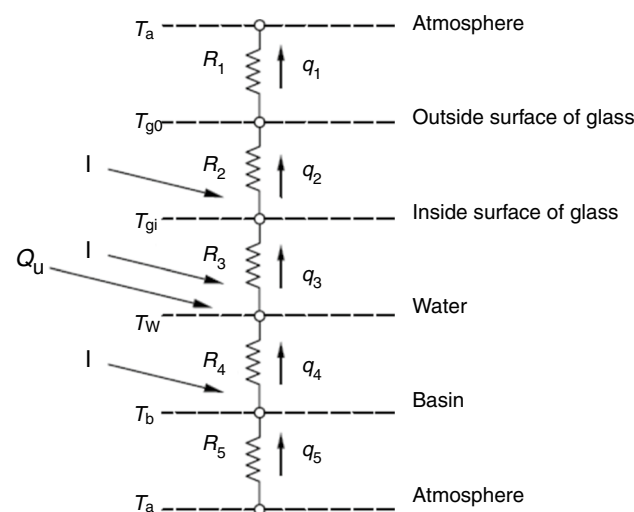
nanofluid and the heat from the basin of the still. Thus, the temperature of the water of the still increases

$$q_3 A_b + Q_{st} = q_4 (A_b - A_{HE}) + q_{abs,3} A_b + Q_u \tag{13}$$

Here,

$$Q_{st} = M_w C_w \frac{dT_w}{dt} \tag{14}$$

$$q_{abs,3} = A_b \alpha'_w I_s(t) \tag{15}$$

$$q_4 = (A_b - A_{HE}) h_w (T_b - T_w) \tag{16}$$

$$Q_u = n \dot{m}_{riser,HE} C_{p,nf} (T_{i,HE} - T_{o,HE}) \tag{17}$$

$q_{abs,3}$ is the heat absorbed in the water from hourly solar radiation. The amount of heat reaching the water from the basin is marked with q_4. The stored energy due to heat received from nanofluid and solar radiation is identified by Q_{st}. The useful energy gain from the heated nanofluid passing through the heat exchanger is Q_u. C_w and $C_{p,nf}$ are the specific heat capacity of water and nanofluid, respectively. To increase the water temperature, all the forms of heat transfer namely conduction, radiation and evaporation plays considerable role. Thus, the total heat transfer coefficient in this case equals to the added values of the conduction, radiation and evaporation heat transfer coefficients.

$$h_{t,wgi} = h_{c,wgi} + h_{r,wgi} + h_{ev,wgi} \tag{18}$$

In Eq. (18), the symbols t, c, r, ev and wgi represent total, conduction, radiation, evaporation and water to glass inside, respectively. The total heat transfer coefficient from water to inner glass surface is denoted by $h_{t,wgi}$. The mass of water in the basin is M_w which can be obtained using Eq. (19)

$$M_w = \rho_w (A_b d_w - V_{HE}) \tag{19}$$

$$\alpha'_w = (1 - \alpha_g)(1 - R_g)(1 - R_w)\alpha_w \tag{20}$$

In Eqs. (19) and (20), A_b, A_{HE} are the surface area of basin and heat Exchanger, respectively. d_w, ρ_w are the depth of water and density of water, respectively. The volume of heat exchanger is V_{HE}. The number of risers of heat exchanger is denoted by 'n'. Absorptivity of water and glass are symbolized with α_w, α_g, respectively. Reflectivity of water and glass are denoted by R_w and R_g, respectively.

The convection heat transfer coefficient h_w between the liner of basin and water is derived from Eq. (21) as follows [29]

$$h_w = \frac{\overline{Nu_L} k_w}{L_c} \tag{21}$$

Here, k_w is thermal conductivity of water and $\overline{Nu_L}$ is the average Nusselt number. L_c is the ratio of surface area to perimeter of the basin

$$\overline{Nu_L} = 0.54 Ra_L^{1/4} \quad \text{when} \quad 10^4 \leq Ra_L \leq 10^7 \tag{22}$$

$$\overline{Nu_L} = 0.15 Ra_L^{1/3} \quad \text{when} \quad 10^7 \leq Ra_L \leq 10^{11} \tag{23}$$

where

$$Ra_L = \frac{g \beta_w (T_b - T_w) L_c^3}{\alpha_{1w} \nu_w} \tag{24}$$

here Ra_L, α_{1w}, β_w, ν_w are Raleigh number, thermal diffusivity, thermal expansion coefficient and kinematic viscosity of the basin water.

Basin liner The basin liner absorbs incident solar radiation. The liner also accepts heat from or rejects heat to the atmosphere

$$q_4 = q_5 + q_{abs,4} \tag{25}$$

Here

$$q_{abs,4} = \alpha'_b I_s(t) \tag{26}$$

$$q_5 = h_b (T_a - T_b) \tag{27}$$

The heat reaching the basin from atmosphere is denoted by q_5 and $q_{abs,4}$ is the absorbed heat because of solar radiation in the basin liner. From Eqs. (26) and (27), the parameters α'_b and h_b can be computed as in Eqs. (28) and (29)

$$\alpha'_b = (1 - \alpha_g)(1 - \alpha_w)(1 - R_g)(1 - R_w)\alpha_b \tag{28}$$

$$h_b = 1/\left(\frac{L_{ins}}{k_{ins}} + \frac{1}{h_{t,b-a}}\right) \tag{29}$$

Here, h_b is the heat transfer coefficient between the basin liner and atmosphere. Insulation thickness and thermal conductivity are represented by L_{ins} and k_{ins}, respectively. Absorptivity of the basin is identified with α_b. The total heat transfer coefficient from basin to atmosphere ($h_{t,b-a}$) is another important parameter which depends on the wind velocity (V_w)

$$h_{t,b-a} = 5.7 + 3.8 V_w \tag{30}$$

Heat exchanger The energy equation for heat exchanger can be stated as Eq. (31)

$$\frac{dT_f}{dx} + C_1 T_f(x) = C_2 \tag{31}$$

Here, the constants C_1 and C_2 can be found using Eqs. (32) and (33) [23]

$$C_1 = \frac{\pi d_{\text{riser,HE}} h_{\text{nf,HE}}}{\dot{m}_{\text{riser,HE}} C_{\text{p,nf}}} \tag{32}$$

$$C_2 = \frac{\pi d_{\text{riser,HE}} \left(h_{\text{nf,HE}} T_w + \frac{\alpha'_{\text{HE}} I_s(t)}{2} \right)}{\dot{m}_{\text{riser,HE}} C_{\text{p,nf}}} \tag{33}$$

Here, $\dot{m}_{\text{riser,HE}}$ and $d_{\text{riser,HE}}$ are the nanofluid mass flow rate and heat exchanger riser diameter, respectively. $C_{\text{p,nf}}$ is the specific heat capacity of nanofluid. The heated nanofluid exchanges heat with the water and the basin liner of the solar still. Temperature of the nanofluid exiting the heat exchanger, $T_{\text{o,HE}}$, can be determined from Eq. (34)

$$T_{\text{o,HE}} = \left(T_{\text{i,HE}} - \frac{C_2}{C_1} \right) e^{-AL_{\text{riser,HE}}} + \frac{C_2}{C_1} \tag{34}$$

Here $T_{\text{i,HE}}$ is the temperature of heated nanofluid entering the heat exchanger. The length of each riser of the heat exchanger is marked by $L_{\text{riser,HE}}$. The coefficient of heat transfer of nanofluid ($h_{\text{nf,HE}}$) flowing to the heat exchanger and the Nusselt number for this flowing fluid can be computed from Eqs. (35) and (36) [23, 29]

$$h_{\text{nf,HE}} = \frac{\text{Nu}_{\text{nf,HE}} k_{\text{nf}}}{d_{\text{riser,HE}}} \tag{35}$$

$$\text{Nu}_{\text{nf,HE}} = 1.86 \left(\text{Re}_{\text{nf,HE}} \text{Pr}_{\text{nf,HE}} \frac{d_{\text{riser,HE}}}{L_{\text{riser,HE}}} \right)^{1/3} \left(\frac{\mu_{\text{nf}}}{\mu_w} \right)^{0.14} \tag{36}$$

Reynolds and Prandtl numbers are two important parameters to compute the heat transfer coefficient and the Nusselt number. These two parameters can be found out by Eqs. (37) and (38) as shown below

$$\text{Re}_{\text{nf,HE}} = \frac{4\dot{m}_{\text{riser,HE}}}{\pi d_{\text{riser,HE}} \mu_{\text{nf}}} \tag{37}$$

$$\text{Pr}_{\text{nf,HE}} = \frac{\mu_{\text{nf}} C_{\text{p,nf}}}{k_{\text{nf}}} \tag{38}$$

Here, Re, Pr, Cp, K and μ represent the Reynolds number, Prandtl number, heat capacity, thermal conductivity and viscosity of the nanofluid flowing through the heat exchanger. Subscripts 'nf' and 'HE' denote Nanofluid and Heat Exchanger, respectively.

Production of distilled water The hourly productivity of pure water m_{pw} in kg m^{-2} h^{-1} unit can be expressed as Eq. (39) [23]

$$m_{\text{pw}} = \frac{3600 h_{\text{ev,w-gi}} (T_w - T_{\text{gi}})}{h_{\text{fg}}} \tag{39}$$

Here, h_{fg} is the latent heat of vaporization of water at temperature of T_w which can be estimated using Eq. (40). Total amount of pure water for a day is nothing but the sum of the hourly amounts of pure water

$$h_{\text{fg}} = 3161.5 - (2.40741 T_w) \tag{40}$$

$$M_{\text{pw}} = \sum m_{\text{pw}} \tag{41}$$

Here M_{pw} is the total amount of distilled water for a day.

First law efficiency The thermal efficiency ($\eta_{\text{th,ss}}$) of solar still is nothing but the ratio of output energy and input energy. In this case, output is the amount of fresh water. So, the output energy is obviously the latent heat given off to produce the fresh water. The thermal efficiency can be estimated either by Eq. (42) or (43) [28]

$$\eta_{\text{th,ss}} = \frac{\sum m_{\text{pw}} x h_{\text{fg}}}{\sum I_s(t) x A_b x \Delta t + Q_{\text{hs}} x \Delta t} \tag{42}$$

Here, Q_{hs} is the power of heat source to heat the nanofluid before entering the heat exchanger. This heat source can be solar energy too. In that case, the heat source Q_{hs} would be replaced by solar collectors to heat the nanofluid. Then, Eq. (42) can be rewritten as Eq. (43) to get the thermal efficiency

$$\eta_{\text{th,ss}} = \frac{\sum m_{\text{pw}} x h_{\text{fg}}}{\sum I_s(t) x A_b x \Delta t + \sum I_{\text{sc}}(t) x A_c x \Delta t} \tag{43}$$

I_s and I_{sc} means the irradiation on the solar still and solar collector, respectively. A_b and A_c are the areas of the basin and solar collector, respectively.

Second law analysis

Exergy efficiency ($\eta_{\text{Ex,ss}}$) is the ratio of output exergy to input exergy as depicted in Eq. (44) [30]. Temperatures of the ambient, the water, the sun and the heat source must be known to compute the exergy efficiency

$$\eta_{\text{Ex,ss}} = \frac{\dot{E}x_{\text{output}}}{\dot{E}x_{\text{input}}} \tag{44}$$

The output exergy is nothing but the evaporative exergy that can be found from Eq. (45)

$$\dot{E}x_{\text{evap}} = \dot{E}x_{\text{output}} = A_b h_{\text{ev,w-g,i}} (T_w - T_{g,i}) \left(1 - \frac{T_a}{T_w}\right) \tag{45}$$

The input exergy ($\dot{E}x_{\text{input}}$) is formed of the combination of solar still and heat source as shown in Eq. (46). The exergy input for solar still is dependent on the incident solar radiation. The power of heat source constitutes the exergy input for heat source

$$\dot{E}x_{\text{input}} = \dot{E}x_{\text{ss}} + \dot{E}x_{\text{hs}} \tag{46}$$

$$\dot{E}x_{\text{ss}} = A_b I_s(t) \left[1 - \frac{4T_a}{3T_{\text{sun}}} + \frac{1}{3}x\left(\frac{T_a}{T_{\text{sun}}}\right)^4\right] \tag{47}$$

$$\dot{E}x_{\text{hs}} = Q_{\text{hs}} \left[1 - \frac{4T_a}{3T_{\text{hs}}} + \frac{1}{3}x\left(\frac{T_a}{T_{\text{hs}}}\right)^4\right] \tag{48}$$

'Ex' stands for exergy. The subscripts 'ss' and 'hs' mean solar still and heat source, respectively. T_a, T_{sun} and T_{hs} are the temperatures of the atmosphere, the sun and heat source, respectively. If solar collector is used to heat the nanofluid, then Q_{hs} would be replaced by $A_c I_s(t)$ and T_{hs} is changed to T_{sun} as written in Eq. (47) to get the input exergy from the heat source.

Numerical solution of the model

The solution for the present model has been carried out numerically by using EES software. In this regard, the nanofluid properties were evaluated first. For a conventional nanofluid with a single nanoparticle in a single base fluid, thermal conductivity can be found following Eq. (49). Thermal conductivity of a hybrid nanofluid with two nanoparticles in a single base fluid can be determined according to the Maxwell model as shown in Eq. (50) and (51) below [31]

$$k_{\text{nf}} = k_{\text{bf}} \frac{k_p + 2k_{\text{bf}} - 2\varphi(k_{\text{bf}} - k_p)}{k_p + 2k_{\text{bf}} + \varphi(k_{\text{bf}} - k_p)} \tag{49}$$

$$k_{\text{hnf}} = k_{\text{bf}} \left[\frac{\frac{(\varphi_{\text{np1}}k_{\text{np1}} + \varphi_{\text{np2}}k_{\text{np2}})}{\varphi_{\text{tot}}} + 2k_{\text{bf}} + 2(\varphi_{\text{np1}}k_{\text{np1}} + \varphi_{\text{np2}}k_{\text{np2}}) - 2\varphi_{\text{tot}}k_{\text{bf}}}{\frac{(\varphi_{\text{np1}}k_{\text{np1}} + \varphi_{\text{np2}}k_{\text{np2}})}{\varphi_{\text{tot}}} + 2k_{\text{bf}} - (\varphi_{\text{np1}}k_{\text{np1}} + \varphi_{\text{np2}}k_{\text{np2}}) + \varphi_{\text{tot}}k_{\text{bf}}}\right] \tag{50}$$

$$\varphi_{\text{tot}} = \varphi_{\text{np1}} + \varphi_{\text{np2}} \tag{51}$$

The Viscosity of any conventional and hybrid nanofluid can be found with the help of Brinkman model as illustrated in Eq. (52) and (53) below [31]

$$\mu_{\text{nf}} = \frac{\mu_{\text{bf}}}{(1 - \varphi)^{2.5}} \tag{52}$$

$$\mu_{\text{hnf}} = \frac{\mu_{\text{bf}}}{\left[1 - (\varphi_{\text{np1}} + \varphi_{\text{np2}})\right]^{2.5}} \tag{53}$$

The specific heat capacity (C_p) and density (ρ) of conventional nanofluid depend on the concentration of the nanoparticle and on the base fluid. The determination of C_p and ρ can be accomplished according to Eqs. (54) and (55) as depicted below [32]

$$\rho_{\text{nf}} = \varphi_{\text{np}}\rho_{\text{np}} + (1 - \varphi_{\text{np}})\rho_{\text{bf}} \tag{54}$$

$$\rho_{\text{nf}}C_{p,\text{nf}} = \varphi_{\text{np}}\rho_{\text{np}}C_{p,\text{np}} + (1 - \varphi_{\text{np}})\rho_{\text{bf}}C_{p,\text{bf}} \tag{55}$$

The specific heat capacity (C_p) and density (ρ) of any hybrid nanofluid depend on the concentration of individual nanoparticles. Analytical expression of C_p and ρ can be represented as in Eqs. (56) and (57) shown below [33]

$$\rho_{\text{hnf}} = \varphi_{\text{np1}}\rho_{\text{np1}} + \varphi_{\text{np2}}\rho_{\text{np2}} + (1 - \varphi_{\text{np1}} - \varphi_{\text{np2}})\rho_{\text{bf}} \tag{56}$$

$$\rho_{\text{hnf}}C_{p,\text{hnf}} = \varphi_{\text{np1}}\rho_{\text{np1}}C_{p,\text{np1}} + \varphi_{\text{np2}}\rho_{\text{np2}}C_{p,\text{np2}} + (1 - \varphi_{\text{np1}} - \varphi_{\text{np2}})\rho_{\text{bf}}C_{p,\text{bf}} \tag{57}$$

Then, the useful heat gain from the nanofluid to the solar still was evaluated by using the temperatures of nanofluid flowing in and out of heat exchanger. Thus, the temperature of the basin water was determined for each time step. At the same time, the relevant heat transfer coefficients were evaluated using the empirical equations given above in Sect. 2.2. Then, the amount of the distillate production was calculated using the heat transfer and thermodynamics relations. Consequently, the first law and the second law efficiencies were evaluated. The flowchart for the numerical solution is shown in Fig. 4.

Fig. 4 Flowchart of the computational solution for the present model
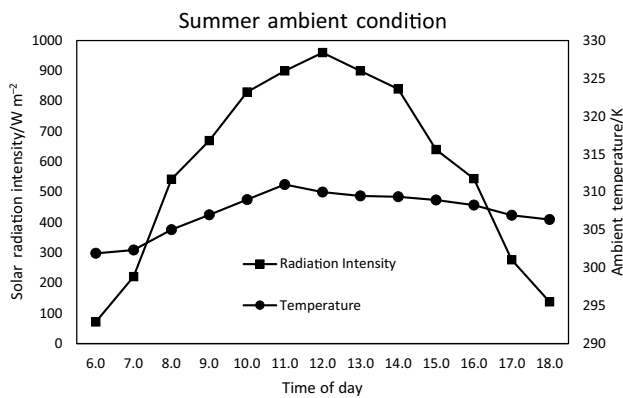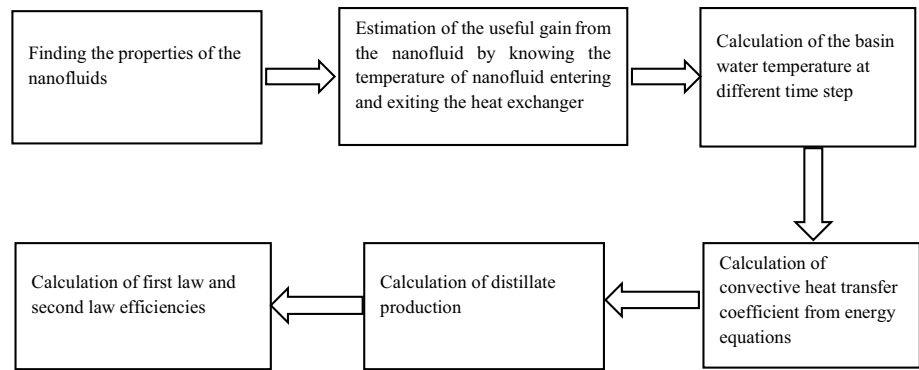

Fig. 5 Solar radiation and ambient temperature of a typical summer day in Dhahran, Kingdom of Saudi Arabia [34]

Table 2 Geometrical dimensions of the solar still

| Parameters	Description	Value
L_{ss}	Length of solar still	1 m
W_{ss}	Width of solar still	0.85 m
d_{head}	Diameter of header of heat exchanger	3.4 cm
dt	Diameter of riser tube of heat exchanger	1.7 cm
L_{riser}	Length of a riser tube	0.77 m

hourly data from 9 am to 3 pm were used in the simulations. Average wind speed is taken as 8 m s^{-1}. The solar radiation and the ambient temperature for a typical summer day at Dhahran are shown in Fig. 5. Table 1 expresses the hourly average solar radiation and temperature of surrounding atmosphere of Dhahran.

The overall geometric dimensions of the solar still are 1 m × 0.85 m. Table 2 below describes the detail geometrical dimensions of the solar still.

Result analysis and discussion

The mathematical model described above is used to assess the characteristics of the solar still equipped with heat exchanger. The performance characteristics presented in this work include the distilled water yield, thermal and exergy efficiencies. Mass flow rate and temperature of nanofluid at inlet of the heat exchanger and depth of basin water were some of the key parameters considered in the current study. The primary objective of the present study is to illustrate the impacts of hybrid nanofluid as heat transfer fluid on the performance characteristics of the solar still. In this regard, the importance of the heat exchanger is illustrated first. Then, the effect of using conventional nanofluid flowing through the heat exchanger is explored. Finally, replacing the conventional nanofluid with the hybrid nanofluid is investigated to show the possible impact of the hybrid nanofluid on the performance characteristics of solar still.

Table 1 Typical summer ambient temperature and hourly average solar radiation data at Dhahran, Saudi Arabia

Time	I/W m^{-2}	Ta/K
09:00	670	307
10:00	830	309
11:00	900	311
12:00	960	310
13:00	900	309
14:00	840	309
15:00	640	308

Experimental data

In the present work, we used the solar radiation, temperature of surrounding atmosphere and speed of wind of a typical summer day at Dhahran, Saudi Arabia as input data for the solar still performance evaluation. Dhahran is situated at 17 meters above the mean sea level in the East of Saudi Arabia. The geographical coordinated of the site are 26.2° N and 50.0° E, respectively. The average

Fig. 6 Comparison of solar still performance with and without heat exchanger at basin water depth, $d_w = 6$ cm
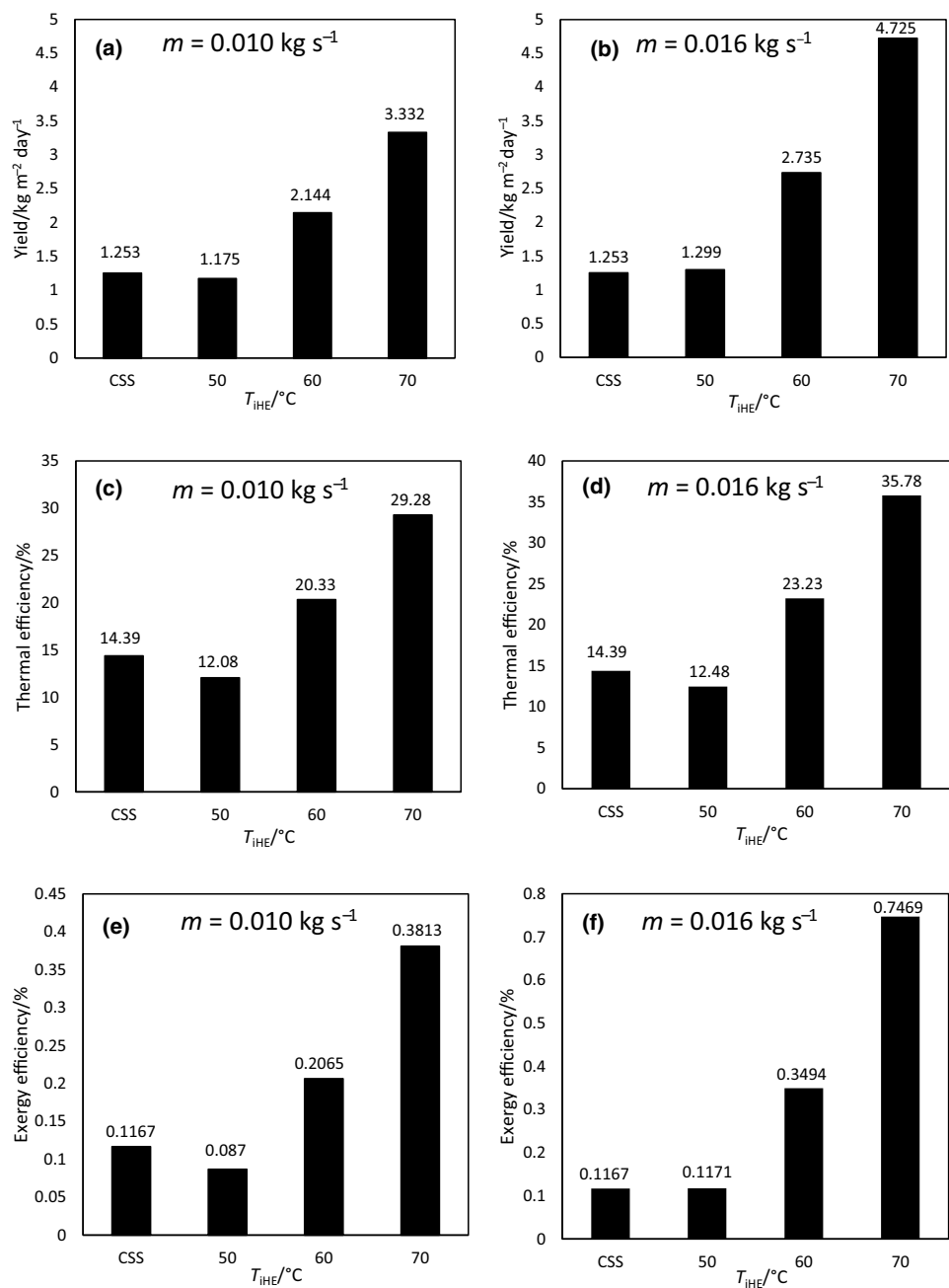
Supplemental heating of the basin water using a heat exchanger raises the water temperature, thus enhances the evaporation rate and thereby increases the yield. Figure 6 provides a comparison of the features of solar still with and without a heat exchanger. Performance characteristics of the conventional solar still (CSS) were compared with the solar still equipped with heat exchanger. Three different inlet temperatures of hot water as heat transfer fluid were considered. The heat exchanger inlet temperatures of the heat transfer fluid were set to be 50, 60, and 70 °C, respectively, as depicted in Fig. 6. The depth of the basin water was fixed at 6 cm. Mass flow rate of 0.01 kg s^{-1}

and 0.016 kg s^{-1} were considered. Figure 6a, b shows the daily yield of distilled water for the conventional solar still and the still equipped with heat exchanger. Incorporating heat exchanger enhances the daily yield except in the case of low inlet temperature of 50 °C and low flow rate of 0.01 kg s^{-1} for which the yield is below the CSS. However, the daily yield improves with the rise in flow rate of hot water as seen in Fig. 6b. The daily yield is found to be nearly four times higher than that of CSS with inlet temperature of hot water (T_{iHE}) of 70 °C and high flow rate (m) of 0.016 kg s^{-1}. Thermal efficiency (Fig. 6c, d) and the exergy efficiency (Fig. 6e, f) also show similar trend
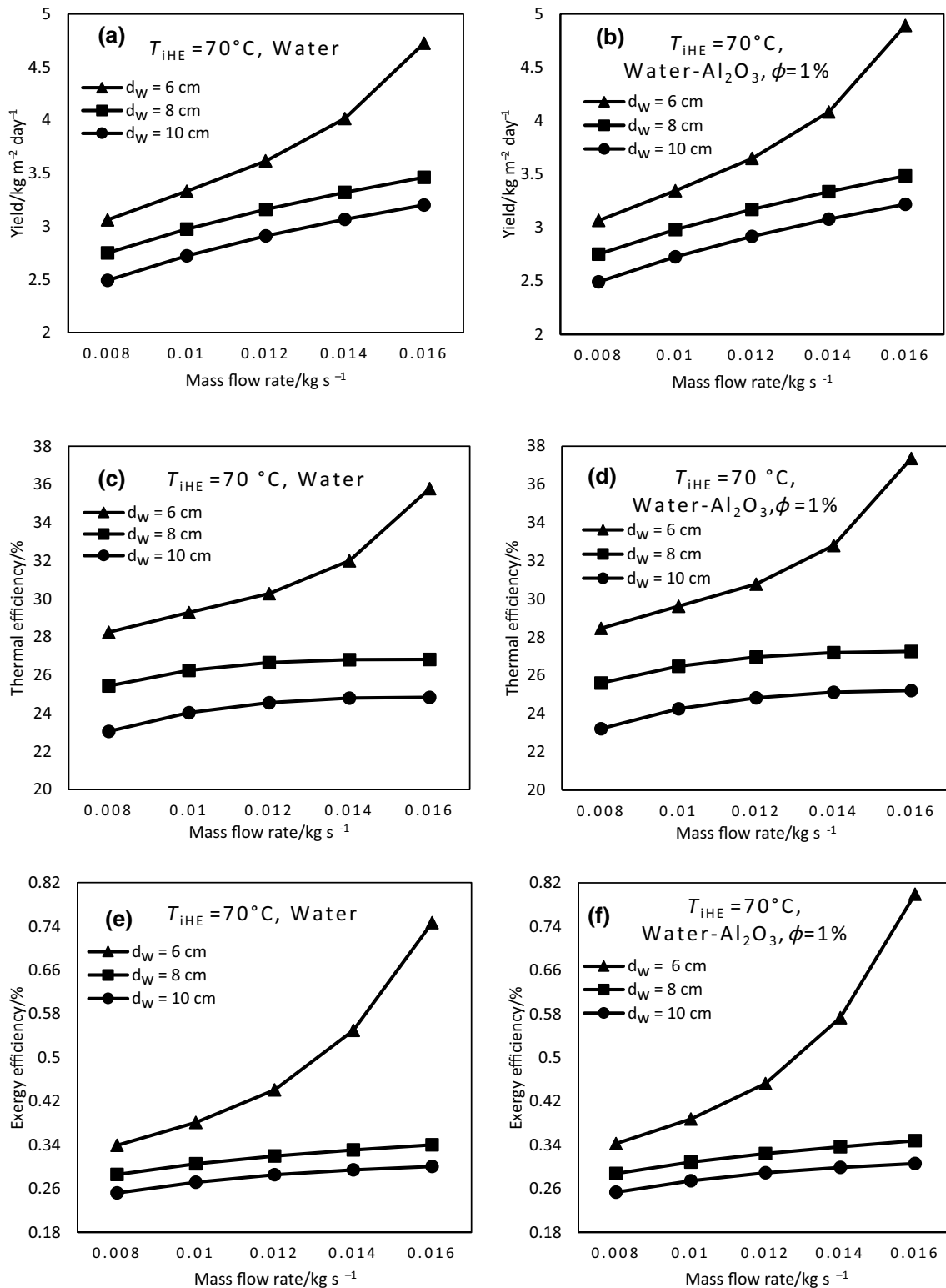
Fig. 7 Comparison of solar still performance between hot water and conventional nanofluid flowing through the heat exchanger

as the daily yield. Both the energy and exergy efficiencies increase considerably when the heat transfer fluid enters into the heat exchanger with a very high temperature and flow rate. The increase in the exergy efficiency is almost sevenfold. Since high inlet fluid temperature increases the performance of the solar still, the inlet temperature

Table 3 Thermophysical properties of nanoparticles used in the analysis

Property	Al_2O_3	CuO	SiO_2
Density/kg m^{-3}	3970	6400	2220
Specific heat/J kg^{-1} K^{-1}	765	531	1000
Thermal conductivity/W m^{-1} K^{-1}	40	76.5	1.38

of heat transfer fluid was kept constant at 70 °C in further analysis.

Use of nanofluids improves the heat transfer characteristics in thermal systems. Compared to hot water, the influence of water–Al_2O_3 nanofluid on the performance of the system is visualized in Fig. 7. The production of pure distilled water increases when water–Al_2O_3 nanofluid is used (Fig. 7b) instead of hot water (Fig. 7a) as heat transfer fluid. The yield increases with the rise of mass flow rate of the nanofluid entering the heat exchanger. It should be noted that the yield remains always high when the depth of water is low (i.e. 6 cm). It is also interesting to note that the increase of the daily pure water yield is considerably higher when the mass flow rate of the fluid (water or nanofluid) inside the heat exchanger increases. This is because of additional heat transfer and further elevation of basin water temperature that results in more evaporation. The energy and exergy efficiencies (Fig. 7c–f) increase when using water–Al_2O_3 nanofluid in the heat exchanger, especially with higher flow rate and lower basin water depth. It should be noted that the enhancement in the exergy efficiency is more pronounced.

The enhancement in heat transfer characteristics that result in the increase of daily pure desalinated water by using nanofluids is due to the thermophysical properties of the nanoparticles such as the specific heat capacity and the thermal conductivity (see Table 3). A comparison of performance parameters when using two different nanofluids, namely water–Al_2O_3 and water–CuO, is presented in Fig. 8. The base case (i.e. the case of hot water as the heat transfer fluid) is also added for comparison. Here, nanofluids water–Al_2O_3 and water–CuO are depicted as NF1 and NF2, respectively. The concentrations for both nanofluids are taken as 1%.

NF1 => water–Al_2O_3 (1% Al_2O_3)
NF2 => water–CuO (1% CuO)

In Fig. 8, the mass flow rate of the fluid is fixed at 0.016 kg s^{-1}, the depth of the basin water is kept at 6 cm and two cases of heat exchanger inlet temperatures (50 °C and 70 °C) are considered. The pure desalinated water yield is considerably higher when the heat exchanger inlet temperature is higher for all cases of heat transfer fluids (Fig. 8a, b). Both nanofluids produced higher daily yield of

pure desalinated water than hot water at T_{iHE} of both 50 °C and 70 °C. The daily pure desalinated water yield with heat exchanger inlet temperature of 50 °C is 1.315 kg m^{-2} day^{-1} for both NF1 and NF2 nanofluid. When the heat exchanger inlet temperature is 70 °C, NF1 yields slightly more desalinated water than NF2. In this case, the daily yield of pure water increases to 4.89 and 4.87 kg m^{-2} day^{-1} for NF1 and NF2, respectively. However, NF2 results in slightly higher thermal efficiency than NF1 (Fig. 8c, d). The thermal efficiency for the case of heat exchanger inlet temperature of 70 °C is 37.3% and 37.5% for NF1 and NF2, respectively. The exergy efficiency shows a similar trend as the daily yield (Fig. 8e, f). The exergy efficiency at T_{iHE} of 70 °C is about 0.8% for both NF1 and NF2.

Hybrid nanofluids offer the possibility of tradeoff between advantages and disadvantages of different nanoparticles. Both the specific heat capacity and the thermal conductivity of nanoparticles are desired to be high for enhancing heat transfer in solar still. Accordingly, in addition to the alumina (Al_2O_3) nanoparticles, two CuO and SiO_2 nanoparticles are considered. As compared with the alumina nanoparticles, CuO has a higher thermal conductivity, and SiO_2 has higher specific heat capacity (Table 3). Thus, we design two hybrid nanofluids by adding CuO and SiO_2 nanoparticles, respectively, to the water–Al_2O_3 nanofluid as follows:

$$HNF1 => Water-Al_2O_3-CuO\left(0.1\% \, Al_2O_3 \quad and \quad 0.1\% \, CuO\right)$$
$$HNF2 => Water-Al_2O_3-SiO_2\left(0.1\% \, Al_2O_3 \quad and \quad 0.1\% \, SiO_2\right)$$

Performance characteristics of the solar still with the hybrid nanofluids HNF1 and HNF2 are shown in Fig. 9. The daily pure desalinated water yield (Fig. 9a, b), the thermal efficiency (Fig. 9c, d) and the exergy efficiency (Fig. 9e, f) improve significantly as the hybrid nanofluid flow rate increases. Improvement of these performance characteristics are more pronounced for basin water depth of 6 cm. To see the influence of hybrid nanofluids on the performance, a comparison of the performance characteristics is given in Fig. 10. In this particular scenario, inlet temperature and the rate of the nanofluid flow were fixed at 70 °C, 0.016 kg s^{-1}, respectively. Basin water depth was kept at 6 cm. The performance comparison of solar still with hot water, NF1, NF2, HNF1, and HNF2 is presented in Fig. 10. The daily pure desalinated water yield is maximum with the hybrid nanofluid HNF2 as seen in Fig. 10a. Pure desalinated water production in this case is 4.991 kg m^{-2} day^{-1}. Thus, the enhancement in the daily yield of pure desalinated water by using the hybrid nanofluid HNF2 is 298.3% compared to CSS. Hybrid nanofluid HNF2 also provides better performance compared to hot water and other conventional nanofluids (NF1 and NF2). The thermal efficiency is maximum (37.76%) when using hybrid nanofluid HNF2 as shown in Fig. 10b. Hybrid nanofluid HNF1 yields slightly
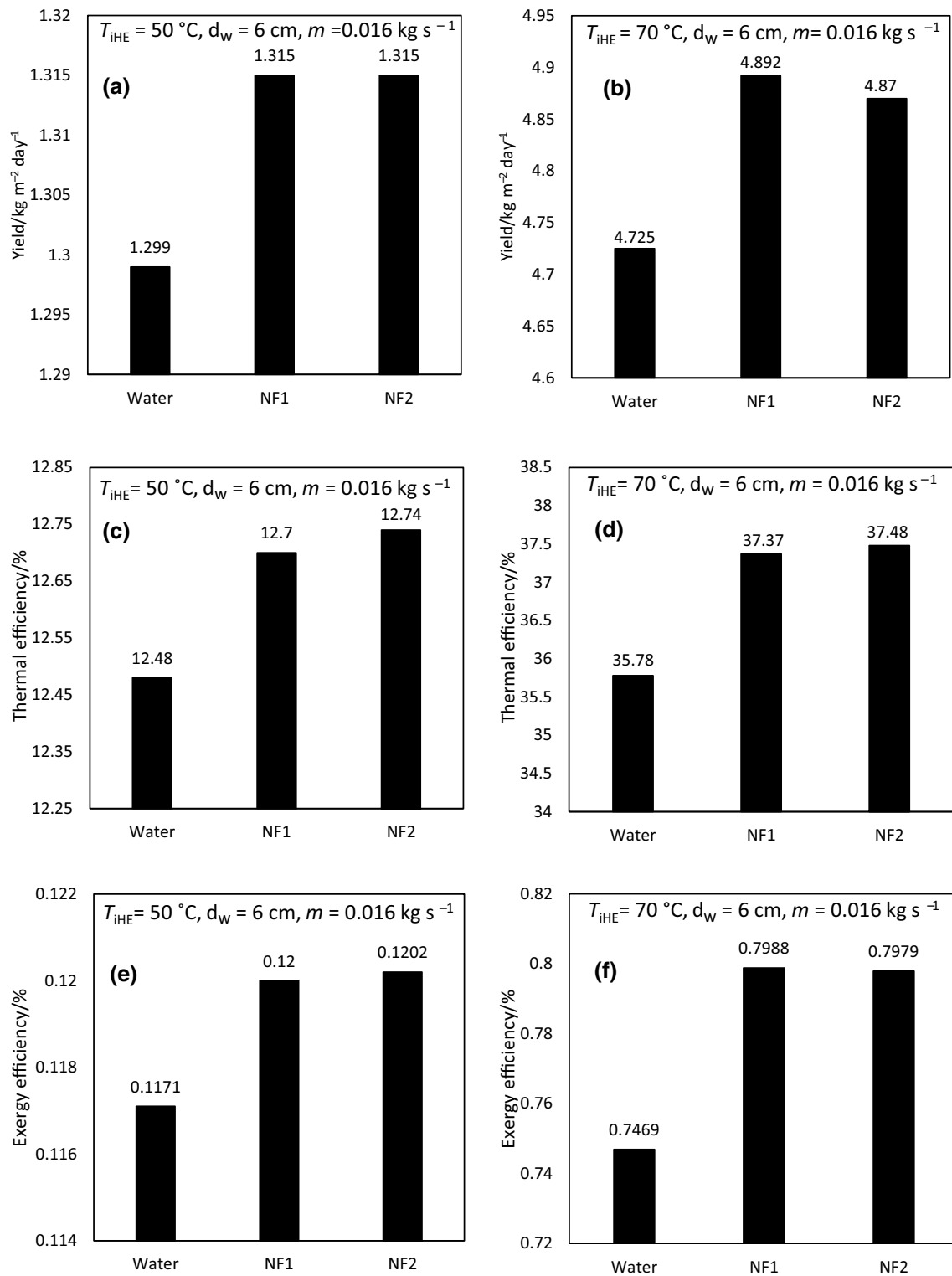
Fig. 8 Comparison of solar still performance with water and conventional nanofluids

higher thermal efficiency than the conventional nanofluids NF1 and NF2. NF2 performed better than NF1 in this case. The superiority of the hybrid nanofluids over the other conventional nanofluids can be clearly seen in Fig. 10c when comparing the exergy efficiencies. Again, the hybrid nanofluid HNF2 showed the highest exergy efficiency (0.82%).
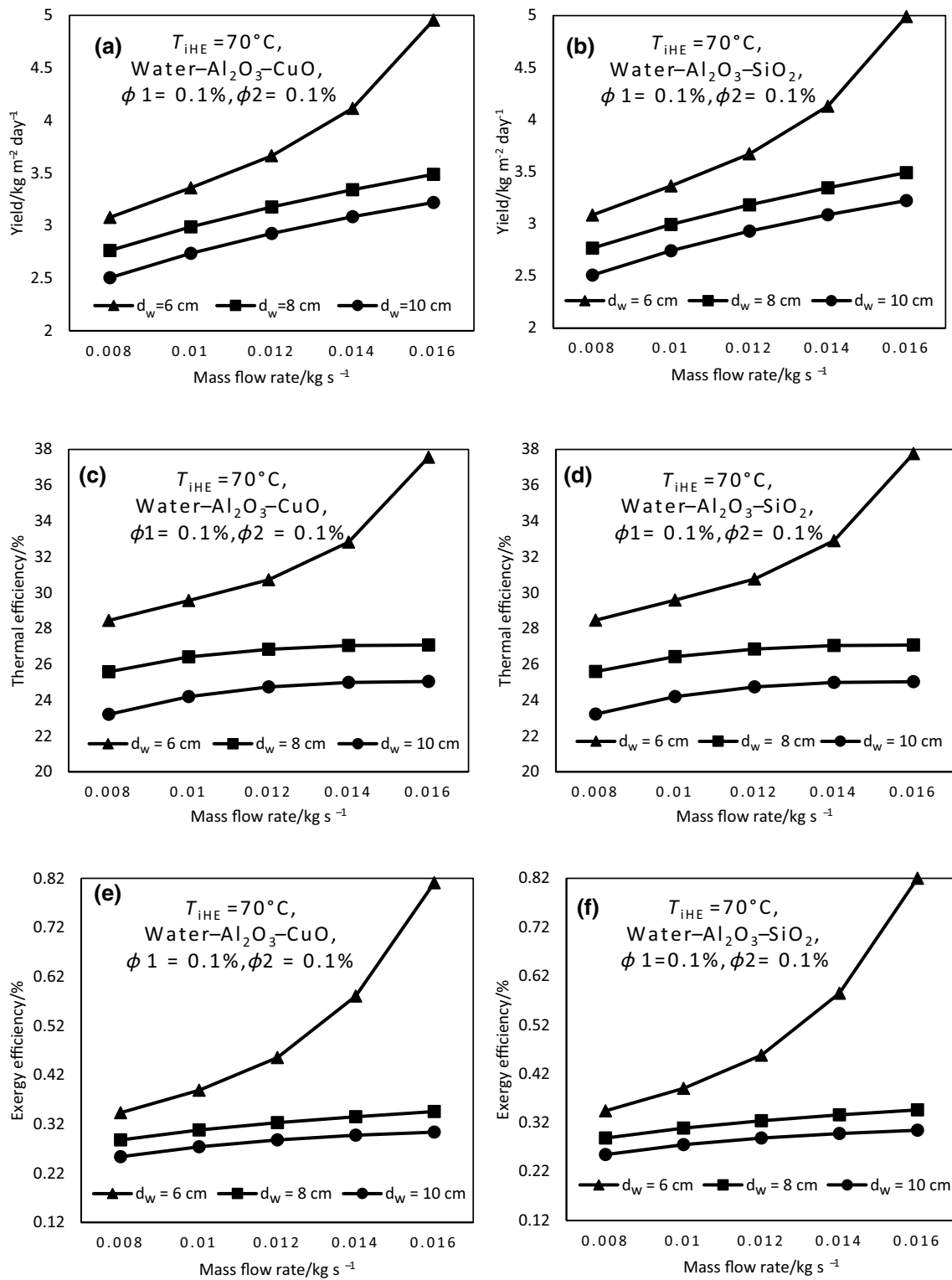
Fig. 9 Performance of solar still with hybrid nanofluids flowing through the heat exchanger

This is followed by the hybrid nanofluid HNF1. The two conventional nanofluids NF1 and NF2 exhibit lower exergy efficiency than hybrid nanofluids but much larger exergy efficiency than hot water.
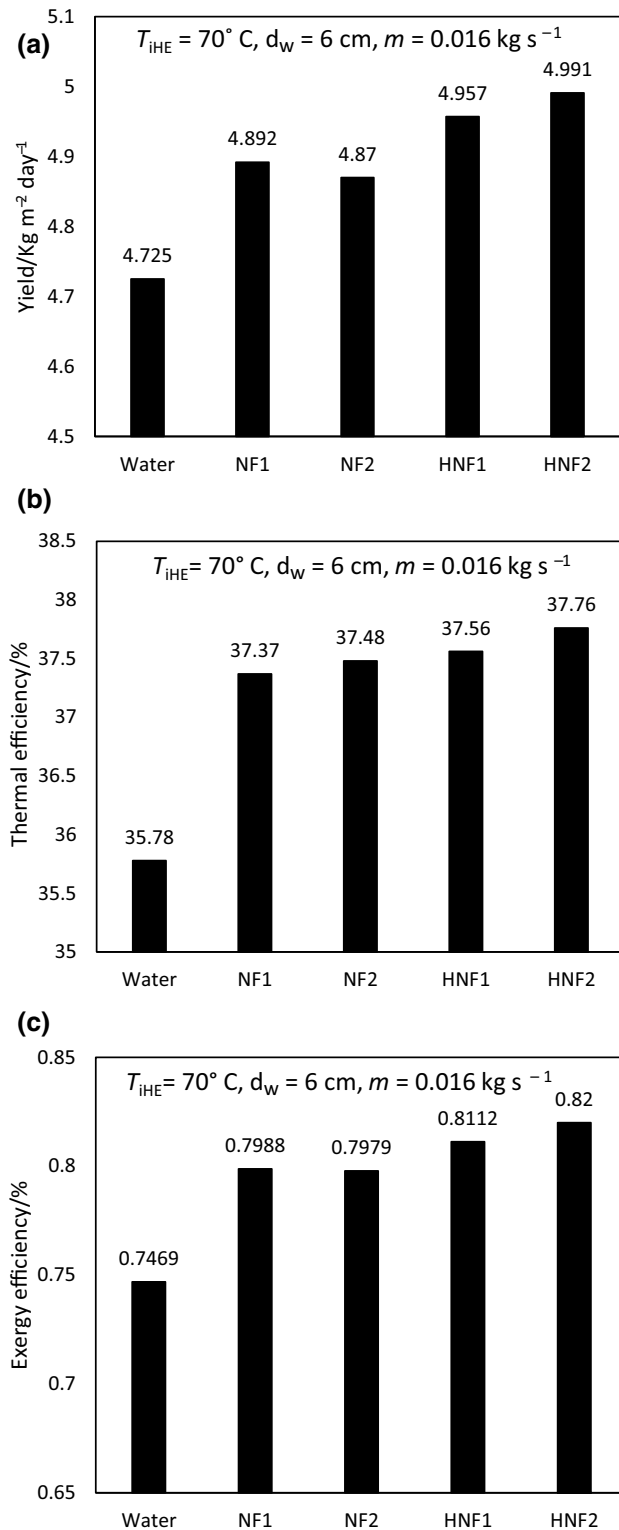
Fig. 10 Performance comparison of solar still with water, conventional nanofluids and hybrid nanofluids flowing through heat exchanger

Conclusions

The performance of solar still fitted with heat exchanger has been analyzed in this study. Hot water and conventional nanofluids were flown through heat exchanger besides hybrid nanofluid to make performance comparison. The mathematical modeling of the modified solar still system is performed using the thermodynamic and heat transfer principles. The performance characteristics such as daily yield of pure distilled water, thermal and the exergy efficiencies were analyzed. First, the performance improvement using a heat exchanger with the solar still is illustrated. Then, the enhancement of the performance using conventional nanofluids in the heat exchanger is studied. Finally, hybrid nanofluids were considered in place of conventional nanofluids and the results for the performance characteristics were compared. The following conclusions can be derived from the present work.

- Heat exchanger enhances the performance of the solar still by improving the pure desalinated water production and efficiency. The higher the temperature of the heat transfer fluid entering the heat exchanger, the better the performance of the solar still.
- Use of nanofluid fluid improves the performance significantly. Daily yield of pure desalinated water using NF1 at 70 °C heat exchanger inlet temperature is as high as 4. 89 kg m^{-2} day^{-1}.
- The daily pure desalinated water yield reaches its maximum of 4.991 kg m^{-2} day^{-1} using water–Al$_2$O$_3$–SiO$_2$ (HNF2) hybrid nanofluid. This corresponds to an enhancement of 298.3% compared to CSS.
- Hybrid nanofluid, HNF2 yields thermal and exergy efficiencies of 37.76% and 0.82%, respectively, making it superior to other nanofluids in this analysis.

In conclusion, it is observed that hybrid nanofluid enhances the performance of the solar still significantly.

References

1. Delyannis AA, Delyannis E. Solar desalination. Desalination. 1984;50:71–81.
2. Izadi M, Oztop HF, Sheremet MA, Mehryan SAM, Abu-Hamdeh N. Coupled FHD–MHD free convection of a hybrid nanoliquid in an inversed T-shaped enclosure occupied by partitioned porous media. Numer Heat Transf Part A Appl (Internet). Taylor and Francis Ltd.; 2019 (cited 2020 Jun

16);76:479–98. Available from: https://www.tandfonline.com/doi/full/10.1080/10407782.2019.1637626.

3. Bayrak F, Ertürk G, Oztop HF. Effects of partial shading on energy and exergy efficiencies for photovoltaic panels. J Clean Prod. 2017;164:58–69.

4. Bayrak F, Oztop HF, Hepbasli A. Energy and exergy analyses of porous baffles inserted solar air heaters for building applications. Energy Build. 2013;57:338–45.

5. Oztop HF, Abu-Nada E. Numerical study of natural convection in partially heated rectangular enclosures filled with nanofluids. Int J Heat Fluid Flow. 2008;29:1326–36.

6. Mahian O, Kianifar A, Kalogirou SA, Pop I, Wongwises S. A review of the applications of nanofluids in solar energy. Int J Heat Mass Transf. 2013;57:582–94.

7. Qu J, Zhang R, Wang Z, Wang Q. Photo-thermal conversion properties of hybrid CuO-MWCNT/H2O nanofluids for direct solar thermal energy harvest. Appl Therm Eng (Internet). Pergamon; 2019 (cited 2019 Mar 10);147:390–8. Available from: https://www.sciencedirect.com/science/article/pii/S1359431118346593.

8. Sahota L, Shyam, Tiwari GN. Energy matrices, enviroeconomic and exergoeconomic analysis of passive double slope solar still with water based nanofluids. Desalination. 2017;409:66–79.

9. Rashidi S, Karimi N, Mahian O, Abolfazli Esfahani J. A concise review on the role of nanoparticles upon the productivity of solar desalination systems. J Therm Anal Calorim. 2019;135:1145–59.

10. Sahota L, Tiwari GN. Exergoeconomic and enviroeconomic analyses of hybrid double slope solar still loaded with nanofluids. Energy Convers Manag (Internet). Pergamon; 2017 (cited 2019 Mar 9);148:413–30. Available from: https://www.sciencedirect.com/science/article/pii/S0196890417305265.

11. Mahian O, Kianifar A, Sahin AZ, Wongwises S. Performance analysis of a minichannel-based solar collector using different nanofluids. Energy Convers Manag (Internet). Pergamon; 2014 (cited 2019 Mar 10);88:129–38. Available from: https://www.sciencedirect.com/science/article/pii/S0196890414007456.

12. Nitiapiruk P, Mahian O, Dalkilic AS, Wongwises S. Performance characteristics of a microchannel heat sink using TiO2/water nanofluid and different thermophysical models. Int Commun Heat Mass Transf (Internet). Pergamon; 2013 (cited 2019 Mar 10);47:98–104. Available from: https://www.sciencedirect.com/science/article/pii/S0735193313001346.

13. Nazari S, Safarzadeh H, Bahiraei M. Performance improvement of a single slope solar still by employing thermoelectric cooling channel and copper oxide nanofluid: an experimental study. J Clean Prod (Internet). Elsevier; 2019 (cited 2019 Mar 9);208:1041–52. Available from: https://www.sciencedirect.com/science/article/pii/S0959652618332165.

14. Nazari S, Safarzadeh H, Bahiraei M. Experimental and analytical investigations of productivity, energy and exergy efficiency of a single slope solar still enhanced with thermoelectric channel and nanofluid. Renew Energy (Internet). Pergamon; 2019 (cited 2019 Mar 9);135:729–44. Available from: https://www.sciencedirect.com/science/article/pii/S0960148118314988.

15. Kabeel AE, Omara ZM, Essa FA. Numerical investigation of modified solar still using nanofluids and external condenser. J Taiwan Inst Chem Eng (Internet). Elsevier; 2017 (cited 2019 Mar 9);75:77–86. Available from: https://www.sciencedirect.com/science/article/pii/S1876107017300305.

16. Kabeel AE, Omara ZM, Essa FA. Enhancement of modified solar still integrated with external condenser using nanofluids: An experimental approach. Energy Convers Manag (Internet). Pergamon; 2014 (cited 2019 Mar 9);78:493–8. Available from: https://www.sciencedirect.com/science/article/pii/S0196890413007346.

17. Rashidi S, Akar S, Bovand M, Ellahi R. Volume of fluid model to simulate the nanofluid flow and entropy generation in a single

slope solar still. Renew Energy (Internet). Pergamon; 2018 (cited 2019 Mar 9);115:400–10. Available from: https://www.sciencedirect.com/science/article/pii/S0960148117308170.

18. Omara AAM, Abuelnuor AAA, Mohammed HA, Khiadani M. Phase change materials (PCMs) for improving solar still productivity: a review. J Therm Anal Calorim. 2020;139:1585–617.

19. Muraleedharan M, Singh H, Udayakumar M, Suresh S. Modified active solar distillation system employing directly absorbing Therminol 55–Al2O3 nano heat transfer fluid and Fresnel lens concentrator. Desalination (Internet). Elsevier; 2019 (cited 2019 Mar 9);457:32–8. Available from: https://www.sciencedirect.com/science/article/pii/S0011916418316369.

20. Shukla DL, Modi KV. Hybrid solar still—liquid desiccant regenerator and water distillation system. Sol Energy (Internet). Pergamon; 2019 (cited 2019 Mar 9);182:117–33. Available from: https://www.sciencedirect.com/science/article/pii/S0038092X19301690.

21. Sharshir SW, Peng G, Wu L, Yang N, Essa FA, Elsheikh AH, et al. Enhancing the solar still performance using nanofluids and glass cover cooling: Experimental study. Appl Therm Eng (Internet). Pergamon; 2017 (cited 2019 Mar 10);113:684–93. Available from: https://www.sciencedirect.com/science/article/pii/S1359431116332227.

22. Elango T, Kannan A, Kalidasa Murugavel K. Performance study on single basin single slope solar still with different water nanofluids. Desalination (Internet). Elsevier; 2015 (cited 2019 Mar 9);360:45–51. Available from: https://www.sciencedirect.com/science/article/pii/S0011916415000089.

23. Mahian O, Kianifar A, Heris SZ, Wen D, Sahin AZ, Wongwises S. Nanofluids effects on the evaporation rate in a solar still equipped with a heat exchanger. Nano Energy. 2017;36:134–55.

24. Sharshir SW, Elkadeem MR, Meng A. Performance enhancement of pyramid solar distiller using nanofluid integrated with v-corrugated absorber and wick: an experimental study. Appl Therm Eng. 2020;168:114848.

25. Parsa SM, Rahbar A, Koleini MH, Aberoumand S, Afrand M, Amidpour M. A renewable energy-driven thermoelectric-utilized solar still with external condenser loaded by silver/nanofluid for simultaneously water disinfection and desalination. Desalination (Internet). Elsevier; 2020 (cited 2020 Feb 22);480:114354. Available from: https://linkinghub.elsevier.com/retrieve/pii/S0011916420300564.

26. Essa FA, Elsheikh AH, Algazzar AA, Sathyamurthy R, Ahmed Ali MK, Elaziz MA, et al. Eco-friendly coffee-based colloid for performance augmentation of solar stills. Process Saf Environ Prot. 2020;136:259–67.

27. Sharshir SW, Kandeal AW, Ismail M, Abdelaziz GB, Kabeel AE, Yang N. Augmentation of a pyramid solar still performance using evacuated tubes and nanofluid: experimental approach. Appl Therm Eng. 2019;160:113997.

28. Tiwari G, Tiwari A. Solar distillation practice for water desalination systems. 2008.

29. Incropera F, NY DD-JWh&SNY. Introduction to heat transfer; 1996.

30. Kianifar A, Zeinali Heris S, Mahian O. Exergy and economic analysis of a pyramid-shaped solar water purification system: active and passive cases. Energy. 2012;38:31–6.

31. Yıldız Ç, Arıcı M, Karabay H. Comparison of a theoretical and experimental thermal conductivity model on the heat transfer performance of Al2O3–SiO2/water hybrid-nanofluid. Int J Heat Mass Transf. 2019;140:598–605.

32. Afzal A, Nawfal I, Mahbubul IM, Kumbar SS. An overviw on the effet of ultrasonication duration on different properties of nanofluids. J Therm Anal Calorim. 2019;135:393–418.

33. Sundar LS, Sharma KV, Singh MK, Sousa ACM. Hybrid nanofluids preparation, thermal properties, heat transfer and friction

factor—a review. Renew Sustain Energy Rev (Internet). Elsevier; 2017;68:185–98. Available from: http://dx.doi.org/10.1016/j.rser.2016.09.108.

34. Antar MA, Zubair SM. Performance evaluation of a solar still in the Eastern Province of Saudi Arabia—an improved analysis. Desalin Water Treat. 2010;22:100–10.